

Automated imaging with ScanLag reveals previously undetectable bacterial growth phenotypes

Irit Levin-Reisman¹, Orit Gefen¹, Ofer Fridman¹,
Irine Ronin¹, David Shwa¹, Hila Sheftel¹ &
Nathalie Q Balaban^{1–3}

We developed an automated system, ScanLag, that measures in parallel the delay in growth (lag time) and growth rate of thousands of cells. Using ScanLag, we detected small subpopulations of bacteria with dramatically increased lag time upon starvation. By screening a library of *Escherichia coli* deletion mutants, we achieved two-dimensional mapping of growth characteristics, which showed that ScanLag enables multidimensional screens for quantitative characterization and identification of rare phenotypic variants.

Systems biology deals mostly with the generation and analysis of large-scale datasets acquired at the molecular level of gene sequences, gene expression and molecular interactions. However, an emerging focus of the systems biology field has been to generate large-scale datasets without compromising on quantitative evaluation of phenotypes¹. The growth rate of microorganisms has always been a crucial phenotypic parameter to monitor², and the search for factors that affect the growth of microorganisms is an active field of study. However, when screening for mutants with growth defects, the discrimination between a delay in growth (referred to as lag time throughout) and slow growth is not always possible. Here we show that our method, ScanLag, enables simultaneous assessment, to the level of a single variant, of lag time and growth rate distributions, thus generating two-dimensional characterization of bacterial populations.

A direct method for measuring the distribution of lag times is to observe single cells under the microscope and monitor the time to first division. A major limitation of this technique is the narrow dynamic time range, as the microcolonies originating from the early growing cells cover the surface at an exponential rate and interfere with the growth of nearby cells. Current methods have overcome this difficulty, using either turbidity measurements or microscopic observations in flow chambers³ but the number of cells that can be tracked is limited, which means the tail of the lag time distribution,

namely the fraction of bacteria that exit the lag phase long after the majority of the population has started growing, cannot be measured. Our goal was to develop an automated method that enables the tail of the lag time and growth rate distributions to be assessed, even for the small fraction of bacteria with very long lag times.

Our method is based on automated measurement of the time it takes for colonies on conventional nutrient agar plates to be detectable, as measured manually in reference 4. To automate this approach^{5,6}, we designed a system comprising an array of commercial scanners⁷ and relays (Fig. 1a and Supplementary Fig. 1) that are directed by our software to periodically acquire images of the colonies growing on plates (Supplementary Software 1). Next, we developed software to automatically analyze the images and extract quantitative parameters, such as the appearance time and growth rate of each colony (Online Methods, Supplementary Software 2, Fig. 1b,c and Supplementary Video 1). We refer to the scanner system and accompanying software as ScanLag and expect it to be implemented easily in other laboratories. A typical lag time distribution produced by ScanLag is shown in Figure 1d.

To determine whether our method indeed measures the lag time of single cells and not later events during the growth of colonies, we compared our results with those obtained using single-cell microscopy. We placed a sample of the bacterial culture on a slide with solid medium and monitored several locations in parallel using an automated microscope system. As mentioned above, considerably fewer single cells can be monitored by this direct method than by ScanLag. Nevertheless, we could compare the distributions obtained from the same culture using single-cell microscopy versus using ScanLag (Fig. 1d). The two distributions overlapped for the most part, except the ScanLag distribution was slightly broader, a feature that theoretical analyses (Supplementary Data and Supplementary Fig. 2) not only explained but predicted to be of the order of the division time. These data support that the late-appearing colonies were delayed because of a long lag and not because of slower colony growth (Supplementary Figs. 3 and 4). Additionally, we checked whether early-appearing colonies influenced the appearance of later colonies. Control experiments confirmed that later appearance was not affected as long as the total number of colonies per plate did not exceed 200 (Online Methods and Supplementary Fig. 5).

Having established the plating density parameters of our system and that ScanLag indeed measures separately lag time and growth rate over thousands of cells, we used ScanLag to characterize the phenotypic heterogeneity of growth rate and lag time, in cultures of wild-type *E. coli*. Phenotypic heterogeneity studies have shed light on the robustness of genetic networks to perturbations⁸ as well as on strategies used by microorganisms to survive under

¹Racah Institute of Physics, The Hebrew University, Edmond J. Safra Campus, Givat-Ram, Jerusalem, Israel. ²Center for Nanoscience and Nanotechnology, The Hebrew University, Edmond J. Safra Campus, Givat-Ram, Jerusalem, Israel. ³Sudarsky Center for Computational Biology, The Hebrew University, Edmond J. Safra Campus, Givat-Ram, Jerusalem, Israel. Correspondence should be addressed to N.Q.B. (nathalieqb@phys.huji.ac.il).

RECEIVED 16 MARCH; ACCEPTED 22 JUNE; PUBLISHED ONLINE 1 AUGUST 2010; DOI:10.1038/NMETH.1485

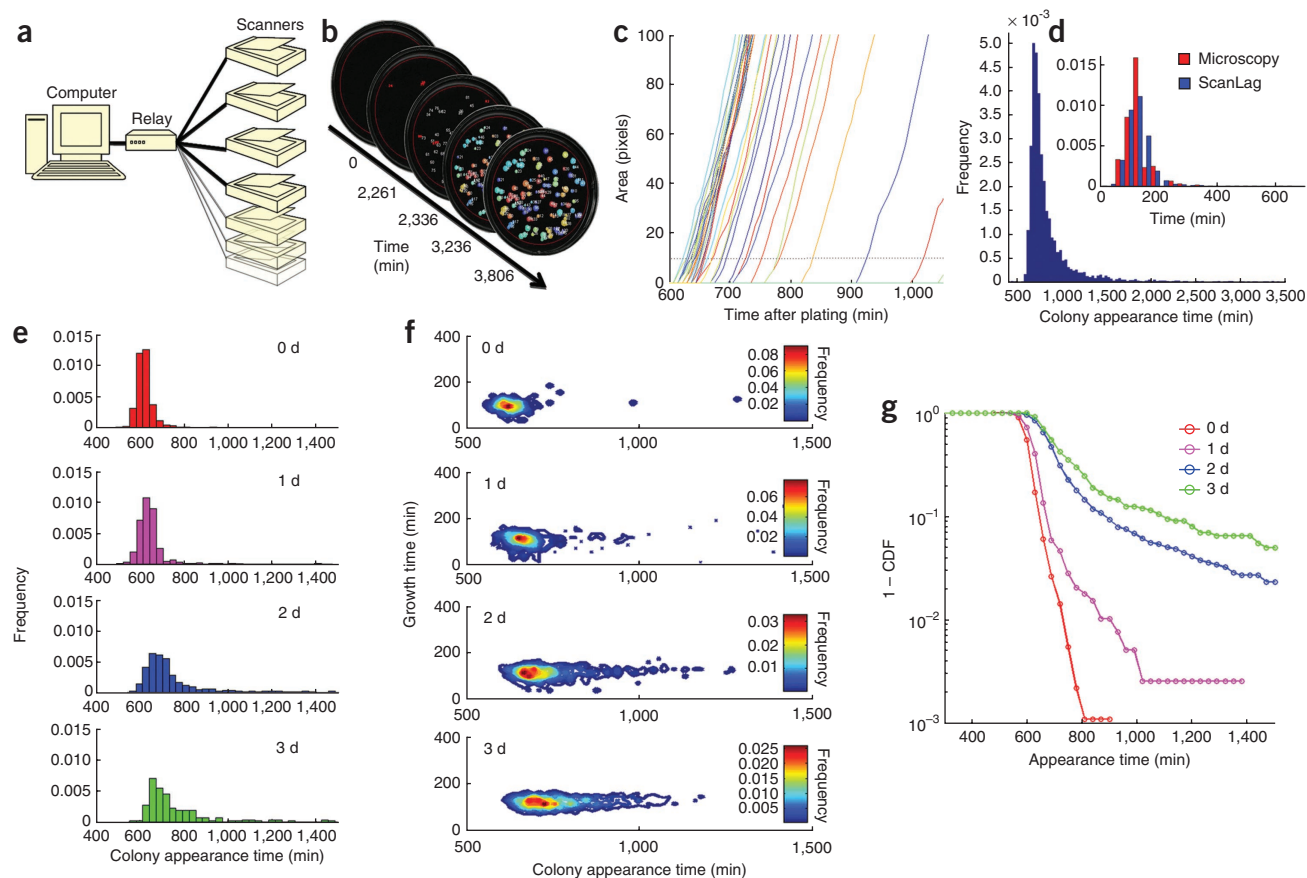


Figure 1 | Lag time and growth rate distribution measurements using ScanLag. **(a)** Experimental setup: an array of scanners is controlled via relays by a computer so that each scanner is periodically turned on and directed to acquire an image of the agar plates. **(b)** Cartoon of automated colony tracking. **(c)** Typical results of ScanLag software analysis of the appearance of colonies on one plate, from a culture starved for 3 d. Lines (arbitrary colors) are plots for individual colonies. The dashed line is the threshold used for detection of appearance. **(d)** Typical distribution of colony appearance times for 5,500 colonies. Inset, lag time distributions in the same culture generated by either single-cell microscopy measurements or ScanLag. **(e)** Lag time distributions of cultures starved for the indicated number of days. **(f)** Histograms of growth rate (defined here by the time taken for a sixfold increase in area size) and colony appearance time for each starvation duration. **(g)** Data from **(e)** represented as one minus cumulative distribution function (1-CDF) on a log scale.

stressful conditions⁹. A striking example of the importance of phenotypic heterogeneity is bacterial persistence after antibiotic treatment¹⁰. It has been found that a subpopulation of bacteria with an extended lag time, generated after the culture has reached stationary phase, survives exposure to multiple antibiotic treatments⁴. In light of this discovery, it has been realized that the distribution of lag times in a bacterial population influences critically the optimal duration of antibiotic treatments. To understand the effect of stationary phase on the subpopulation of bacteria with long lag times, we used ScanLag to compare the lag distribution in bacteria that have been at stationary phase for different durations. We grew bacterial cultures to stationary phase; daily, we plated a sample of this culture and monitored lag time and growth rate using ScanLag. We repeated this protocol for different starvation conditions (Online Methods). In all conditions tested, the mean time of colony appearance correlated with the duration of starvation (**Fig. 1e**). Our data were consistent with those generated in previous studies^{5,11–13}, but owing to the high resolution and the two-dimensional mapping enabled by ScanLag, we delineated that the main effect of longer starvation duration was to increase the magnitude of the tail of the lag time distribution (**Fig. 1f,g**). Although the mean lag time increased at most by a factor of two with prolonged starvation duration, the size of the subpopulation

with an extended lag time increased by more than an order of magnitude (**Fig. 1g**). Thus, using ScanLag we found that starvation in conventional liquid and solid media resulted in more bacteria remaining dormant for longer periods, which accounted for the positive correlation between the magnitude of the lag time distribution tail and the number of bacteria surviving antibiotic treatments because antibiotics are less potent against nongrowing bacteria (**Supplementary Fig. 6**). We verified, by regrowing colonies that appeared late, that the tail of the lag distribution was not due to genetic changes (**Supplementary Fig. 7**).

Next we used ScanLag to survey the growth characteristics of the library of large deletions in *E. coli*¹⁴. Based on the concomitant measurement of growth rate and lag time distributions, we classified the deletion mutants into four new phenotypic classes, as illustrated by four representative strains (**Fig. 2**), separated clearly on the two-dimensional histogram: (i) normal growers, normal lag (wild-type phenotype), (ii) normal growers, long lag, (iii) bimodal lag and (iv) slow growers. The two-dimensional mapping generated by ScanLag allowed us to determine whether growth rate and lag are correlated. For example, the bimodality we observed in mutant strain number 5053 originated from a bimodality of lag times. Additional analysis of these growth phenotypes should explain their genetic basis.

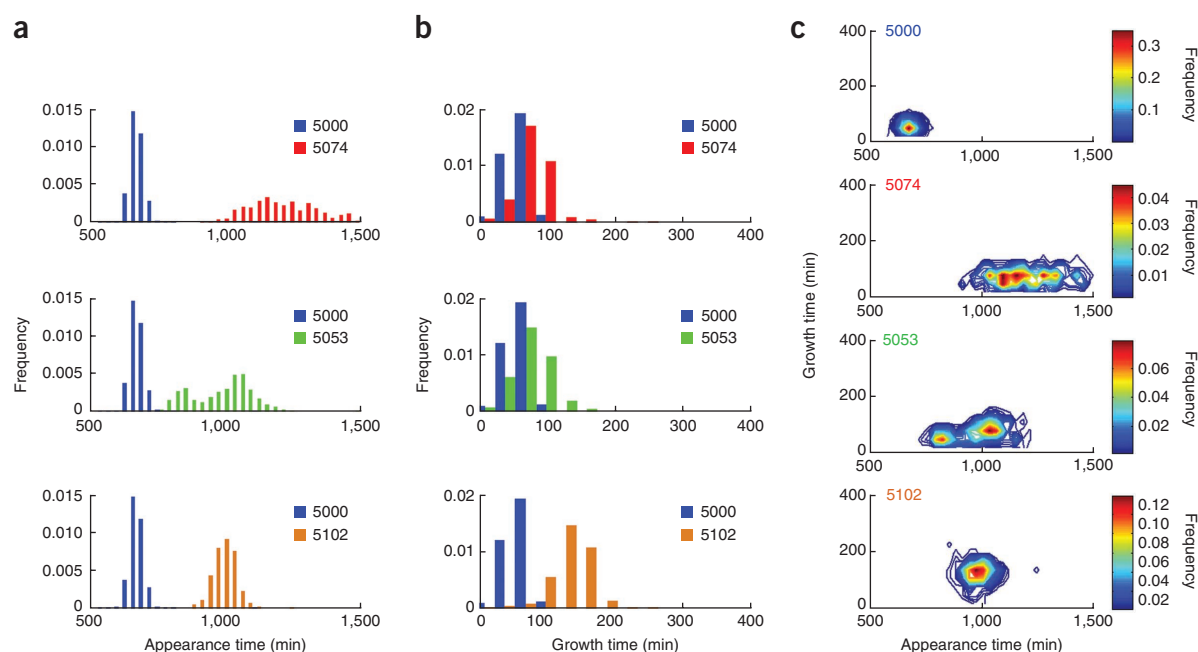


Figure 2 | Two-dimensional mapping of the *E. coli* library of long deletions using ScanLag. **(a)** Lag time distributions for four representative strains. The 5000 strain is the wild type. **(b)** Area growth rate distributions for the same strains as in **a**. **(c)** Histograms of the growth and lag distributions. Compared to the wild type (strain 5000), the 5074 mutant strain had very late appearance time but normal growth; the 5053 mutant strain exhibited bimodal appearance time; and the 5102 mutant strain appeared late mostly due to reduced growth rate.

Using Scanlag, we studied, to our knowledge for the first time, the tail of the lag time distribution of wild-type *E. coli*. Bacteria with a long lag time are protected from many antibiotics and other stresses that kill actively growing cells⁴. Colonies founded from these ‘persistent’ bacteria started growing several days after plating, considerably later than typical incubation time used in survival assays (Fig. 1g). This phenomenon could underlie the ‘viable but not culturable’ phenotype¹⁵, in which metabolically active bacteria do not form colonies on plates.

ScanLag can be adapted to measure other parameters such as colony morphology and color, and thus can be used for multi-dimensional mapping. Moreover, apart from revealing new phenotypes that cannot be measured by population-level measurements, ScanLag enables the identification and retrieval of rare mutants. For example, after plating a mutagenized population, mutants can be characterized phenotypically and isolated directly, even without using selective conditions. Therefore, we expect that ScanLag will be a powerful tool for facilitating various screens. We anticipate that the multidimensional information uncovered by future experiments using ScanLag will lead to better characterization of microbial populations, important for both medical and environmental research.

METHODS

Methods and any associated references are available in the online version of the paper at <http://www.nature.com/naturemethods/>.

Note: Supplementary information is available on the Nature Methods website.

ACKNOWLEDGMENTS

We thank A. Keynan for invaluable discussions on the importance of the lag phase, D. Azulay and A. Bar-Yaacov for helpful theoretical discussions, I. Rosenshine (Hebrew University) for strains, and the National BioResource Project and National Institute of Genetics, Japan for the large and medium

deletion mutants library, S. Silbert for initial software development and E. Rotem and S. Pearl for technical support and comments on the manuscript. The work was supported by the Human Frontier Science Program and by the Israel Science Foundation.

AUTHOR CONTRIBUTIONS

I.L.-R., O.G., I.R. and D.S. performed the research. O.F. and H.S. contributed analytical tools. N.Q.B., I.L.-R., I.R. and O.G. designed the research. N.Q.B. wrote the paper.

COMPETING FINANCIAL INTERESTS

The authors declare no competing financial interests.

Published online at <http://www.nature.com/naturemethods/>.

Reprints and permissions information is available online at <http://npg.nature.com/reprintsandpermissions/>.

- Collins, S.R., Weissman, J.S. & Krogan, N.J. *Nat. Methods* **6**, 721–723 (2009).
- Bochner, B.R. *FEMS Microbiol. Rev.* **33**, 191–205 (2009).
- Elfving, A., LeMarc, Y., Baranyi, J. & Ballagi, A. *Appl. Environ. Microbiol.* **70**, 675–678 (2004).
- Balaban, N.Q., Merrin, J., Chait, R., Kowalik, L. & Leibler, S. *Science* **305**, 1622–1625 (2004).
- Guillier, L., Pardon, P. & Augustin, J.C. *Appl. Environ. Microbiol.* **71**, 2940–2948 (2005).
- Glaser, D.A. & Wattenburg, W.H. *Ann. NY Acad. Sci.* **139**, 243–257 (1966).
- Michel, J.B., Yeh, P.J., Chait, R., Moellering, R.C. & Kishony, R. *Proc. Natl. Acad. Sci. USA* **105**, 14918–14923 (2008).
- Barkai, N. & Shilo, B.Z. *Mol. Cell* **28**, 755–760 (2007).
- Dubnau, D. & Losick, R. *Mol. Microbiol.* **61**, 564–572 (2006).
- Bigger, J.W. *Lancet* **244**, 497–500 (1944).
- Hershey, A.D. *J. Bacteriol.* **37**, 285–299 (1939).
- Pin, C. & Baranyi, J. *Appl. Environ. Microbiol.* **74**, 2534–2536 (2008).
- Niven, G.W., Morton, J.S., Fuks, T. & Mackey, B.A. *Appl. Environ. Microbiol.* **74**, 3757–3763 (2008).
- Kato, J. & Hashimoto, M. *Mol. Syst. Biol.* **3**, 132 (2007).
- Kapelyants, A.S. *et al. Intercellular Signalling and the Multiplication of Prokaryotes: Bacterial Cytokines* (Cambridge University Press, 1999).

ONLINE METHODS

Time-lapse scanning. We wrote an automated periodical image acquisition application, in Microsoft.Net framework (C# language) using Windows Image Acquisition (WIA) standard interface. This application controlled a scalable number of scanners. The application is generic enough to work with any type of scanner supported under Microsoft Operating systems (through the WIA interface).

To measure the lag distributions reliably, several difficulties had to be overcome. First, despite a temperature controlled environment, we observed important temperature gradients across the surface of the scanners due to the heating up of the electronics. This resulted in different growth conditions at the different locations (Supplementary Fig. 1a). To overcome this problem, we implemented an optional module in the application that includes a power management mechanism to control the scanner components that heat up upon usage (such as lamps and motors), which may change the temperature in their proximity. This is achieved by turning on these components only when a scan is performed. Additional hardware was required in cases where disabling the USB interface was not sufficient, in which case the scanner's on-off switch was bypassed using a relay that was controlled by the application. Using the power management application, we reached a temperature uniformity of $\pm 0.2^\circ\text{C}$, as measured by an array of thermocouples that were placed at different locations across the scanner surface (Supplementary Fig. 1b), as well as between scanners.

Second, scanners are designed to be used on thin objects (such as paper or film) that lie directly on the glass surface, whereas Petri dishes have volume. Even though the colonies themselves lie on top of the agar layer, about 5 mm above the scanner surface, they are still within the scanner's field of depth and thus are in focus. Still, the edges of the Petri dish may appear in the image, depending on the location of the charge-coupled devices (CCDs) in the scanner. These edges can interfere with the automated analysis of the colonies in the images. To avoid colony growth where these edges project, the plating area was limited to a smaller inner circle using sterile Delrin rings.

Third, to gain good contrast between the colonies and the dish, a black felt cloth was used as background, placed between the Petri dish and its lid. This felt cloth also absorbed the moisture that accumulated on the plastic lid, which otherwise would have condensed and dripped in the Petri dish and disrupted the growth of colonies.

Image analysis. The goal of the image analysis software is to detect and track the colonies while extracting quantitative parameters such as size and growth rate for each colony over time. We wrote an image-processing application using Matlab (MathWorks). The application consists of three stages: (i) preprocessing of the images, (ii) detection and tracking of the colonies and (iii) analysis of the extracted data.

Preprocessing. The images from the scanner are aligned to each other. For each Petri dish, its location is detected in the first image and then cropped from the sequence of images. The time axis is retrieved from the timestamp of each image.

Detection and tracking. For every image of each Petri dish, the image is first converted to grayscale, and then the background is

subtracted. Pixels above a certain gray level threshold are detected, clustered into colonies and assigned an identifying number. The tracking of colonies over time was achieved through the overlap between objects in subsequent images. The output of this process resulted in tables containing each colony's area (number of active pixels) and center of 'mass' (center of brightness) from every image (Fig. 1b,c and Supplementary Video 1).

Analysis of the extracted data. The colony appearance time was measured for each colony, namely the time at which the colony size exceeded a threshold of typically ten pixels. We verified that the colony appearance distributions were not affected by changing this threshold (Supplementary Fig. 4).

Evaluation of maximal plating density for lag measurements.

To determine whether early-appearing colonies influenced the appearance of later colonies, we used one strain with a short mean lag time and another cold-sensitive strain whose growth lag time can be set by growth temperature. The distribution of appearance of each strain was the same irrespective of whether the strains were plated alone or together (Supplementary Fig. 5). This showed that the early appearance of colonies of the fast strain does not affect the later appearance of the delayed colonies. Repeating this experiment at different plating densities revealed that the later appearance was not affected as long as the total number of colonies per plate did not exceed 200.

Media and chemicals. M9 (Difco M9 minimal salts, 5 \times) with 0.1% amino acids was used as liquid growth medium. LB Difco LB broth Bacto agar was used as solid growth medium. Kanamycin (Sigma) at 30 $\mu\text{g ml}^{-1}$ was added to all media. Serial dilutions were performed in 0.9% NaCl for bacterial plating. Ampicillin (Sigma) at 20 $\mu\text{g ml}^{-1}$, streptomycin (Sigma) at 50 $\mu\text{g ml}^{-1}$ and anhydrous tetracycline (Acros Organics) at 0.2 $\mu\text{g ml}^{-1}$ were used for microscopy experiments. Ampicillin at 100 $\mu\text{g ml}^{-1}$ and penicillinase (Sigma) at 1 unit ml^{-1} were used for the survival assay.

Bacterial strains and plasmids. *lacI* and *tetR* genes were transduced using P1_{vir} lysate of DH5 α Z1 into strains MGY and MGYA7 (ref. 4) to create MGYZ1 and MGYA7Z1, respectively. *E. coli* strain DH5 α Z1 was obtained from H. Bujard (University of Heidelberg)¹⁶. The plasmid pZA21mCherry, carrying *mCherry* under the *Tet* promoter has been described previously¹⁷. The Keio collection of large chromosomal deletions¹⁴ in *E. coli* was obtained from National BioResource Project (NBRG) National Institute of Genetics (NIG) Japan).

Growth conditions. Single colonies were diluted into fresh LB medium with the appropriate antibiotics. Cells were grown overnight at 37 $^\circ\text{C}$, with shaking. Cultures referred to as frozen stock were supplied with 15% glycerol and stored at -80°C . The overnight-frozen stock was starved using two methods: liquid medium or solid medium. In liquid medium, the overnight-frozen stock was diluted into fresh M9 with 0.1% amino acids and the appropriate antibiotics, and grown at 37 $^\circ\text{C}$, with shaking. After the culture reached stationary phase, samples were frozen with 15% glycerol at several time points. On solid medium, the overnight-frozen stock was serially diluted in 0.9% NaCl and plated on LB-kanamycin plates at 37 $^\circ\text{C}$. Colonies formed were picked, suspended



and diluted in 0.9% NaCl at several time points. Starved cultures from both liquid and solid media were examined as described below. Large and medium deletions collection cultures (NIG, Japan) were grown in LB-streptomycin with 15% glycerol overnight at 37 °C, with shaking. The overnight culture was diluted 1:1,000 in M9 with 0.1% amino acids and streptomycin and grown overnight. After the culture reached stationary phase, samples were frozen with 15% glycerol.

Scanning procedure. A culture was plated on LB agar Petri dishes with appropriate antibiotics, and the Petri dishes were scanned (Epson Perfection 3490 and Epson Perfection v200) at 32 °C, automatically and serially. The images were taken at 300 dots per inch (d.p.i.).

Survival assay. A culture was diluted into a beaker with fresh LB and ampicillin at 32 °C, with shaking. Samples were taken at several time points. Each sample was supplied with penicillinase to neutralize the ampicillin. The number of bacteria in the culture was determined by the most probable number-counting method^{18,19}.

Single-cell microscopy: observation chambers. A polydimethylsiloxane (PDMS) square mold was cut out of cured Sylgard 184 (Dow Corning) layer (thickness: ~2 mm). The mold was filled with melted LB agarose with low concentration of ampicillin (20 µg ml⁻¹) and anhydrous tetracycline (0.2 µg ml⁻¹). Bacteria (2 µl) were put on a coverslip (number 1.5) and covered with the

solidified LB-agarose inside the PDMS mold. The whole chamber was sealed with a thin layer of PDMS to avoid dehydration of the LB-agarose, without blocking oxygenation.

Time-lapse microscopy. The PDMS chambers were monitored using a Leica DMIRBE inverted microscope system with incubator box (Life Imaging Systems), automated stage and shutters. Autofocus and image acquisition was done using custom macros in ImagePro/Scope-Pro (Media Cybernetics) to control the microscope, stage, shutters and camera. Multiple locations were monitored in parallel for phase-contrast and fluorescence imaging of the same chamber. Images were acquired using a 100× long-range oil objective and a cooled CCD camera (Orca; Hamamatsu). Microscopy was carried out at 32 °C.

Microfluidics. The microfluidic devices were fabricated as previously described⁴. Briefly, the microfluidic devices consist of several layers clamped together: a thin patterned PDMS layer (Sylgard 184; Dow Corning) with microscopic grooves or rectangular boxes made by soft lithography techniques²⁰ using a mold of AZ4110 (Clariant); a cellulose membrane; and a thicker PDMS layer with flow channels patterned using a mold of SU-8 2100 (MicroChem).

16. Lutz, R. & Bujard, H. *Nucleic Acids Res.* **25**, 1203–1210 (1997).
17. Gefen, O., Gabay, C., Mumcuoglu, M., Engel, G. & Balaban, N.Q. *Proc. Natl. Acad. Sci. USA* **105**, 6145–6149 (2008).
18. Hurley, M.A. & Roscoe, M.E. *J. Appl. Bacteriol.* **55**, 159–164 (1983).
19. Cochran, W.G. *Biometrics* **6**, 105–116 (1950).
20. Quake, S.R. & Scherer, A. *Science* **290**, 1536–1540 (2000).